Thermal Memory of Polyethylenes Analyzed by Temperature Modulated Differential Scanning Calorimetry

G. Amarasinghe, F. Chen, A. Genovese, R. A. Shanks

Department of Applied Chemistry, RMIT University, GPO Box 2467V, Melbourne, Victoria 3001, Australia

Received 22 November 2002; accepted 6 February 2003

ABSTRACT: Temperature modulated differential scanning calorimetry (TMDSC) was employed to study the melting and crystallization behavior of various polyethylenes (PEs). Samples of high density PE (HDPE), low density PE (LDPE), linear low density PE (LLDPE), and very low density PE (VLDPE) with different crystal structures and morphologies were prepared by various thermal treatments (isothermal crystallization and slow, fast, and dynamic cooling). The reversing and nonreversing contributions, measured on the experimental time scale, were varied, depending on the crystal stability. A relatively large reversing melt contribution occurs for unstable crystals formed by fast cooling compared to those from slow cooling treatments. All samples of highly branched LDPE, LLDPE, and VLDPE showed a broad exotherm before the main melting peak in the nonreversing curve, suggesting crystallization and annealing of crystals to more stable forms. Other samples of HDPE, except when cooled quickly, did not show any significant crystallization and annealing before melting. The crystallinity indicated that dynamically cooled polymers were much more crystalline, which can be attributed to crystal perfection at the lamellar surface. A reversible melting component was also detected during the quasiisothermal TMDSC measurements. Melting is often accompanied by large irreversible effects, such as crystallization and annealing, where the crystals are not at equilibrium. Such phenomena during a TMDSC scan provide information on the polymer thermal history. © 2003 Wiley Periodicals, Inc. J Appl Polym Sci 90: 681–692, 2003

Key words: polyethylene; crystallization; melting; differential scanning calorimetry; temperature modulated differential scanning calorimetry

INTRODUCTION

The melting of a polymer is generally a complex process because the polymer crystal structure undergoes various transformations, such as recrystallization, annealing, and perfection during scanning.[1] Differential scanning calorimetry (DSC) has long been a valuable technique that is used to study melting and crystallization behavior and the morphology of polymers. The temperature range of melting in a DSC scan is indicative of the size and perfection of the crystallites in the sample. Nevertheless, temperature modulated DSC (TMDSC), which uses a periodical temperature modulation over a traditional linear heating or cooling ramp, is a more powerful method with the capability of giving more information than conventional DSC.[2,3] It is capable of measuring the underlying kinetic and thermodynamic processes of a sample during temperature scanning and offers added advantages over conventional DSC by separating overlapping transitions with improved sensitivity and resolution. Because of these characteristics of the TMDSC technique, it can be regarded as a useful tool to study various thermal transitions including the glass transition, melting, and crystallization of polymers.[4–6] TMDSC has recently been used for the analysis of the melting of many polymers including poly(ethylene terephthalate) (PET),[7–9] poly(oxyethylene),[10,11] polyethylenes (PEs),[12–16] polypropylene,[17,18] poly[carbonyl(ethylene-*co*-propylene)],[19] poly(ethylene 2,6-napthalenedicarboxylate),[20,21] and multiblock copolymers.[22]

Regardless of the instrument used, several types of curves can be derived from a TMDSC experiment.[23] The in-phase component, which is the reversing or storage heat flow or heat capacity (C_p'), represents the heat effects that are reversible at the time and temperature of modulation. The value of C_p' is calculated from the amplitude of the first harmonic of the Fourier transformation series of heat flow versus time. Thus, it does not contain all thermal effects that are fully reversible, instead containing only a portion of the reversible processes that occur within the modulation amplitude. The out of phase component, which is the loss or kinetic heat capacity (C_p''), is expected to show the heat flow that has resulted from kinetic effects at the time and temperature at which they are detected. The in-phase/out of phase approach is difficult to interpret, so results have been presented in terms of reversing/nonreversing processes, which can also be described as an in-frequency/out of frequency ap-

Correspondence to: R. A. Shanks (robert.shanks@rmit.edu.au).

Journal of Applied Polymer Science, Vol. 90, 681–692 (2003)

proach. The total heat flow obtained by dividing the average heat flow by the average heating rate is equal to the heat flow from conventional DSC. Other signals, the nonreversing component ($C_{p\mathrm{NR}}$), which is also primarily considered to reflect only irreversible phenomena, are obtained by subtracting reversing heat flow from the total heat flow. The glass transition is always reversible; however, the relaxation enthalpy associated with the glass transition is irreversible. Changes such as crystallization and curing reactions are often irreversible. The glass transition always appears in the total C_p and C_p' curves. The exothermic changes corresponding to the enthalpy of relaxation, crystallization, and chemical reactions only appear in the total C_p and $C_{p\mathrm{NR}}$ curves, not in the C_p' curve. Nevertheless, the process of melting is mostly thermodynamically reversible with a nonreversing character associated with recrystallization, crystal annealing, and perfection of the nonequilibrium crystals during the melting that can be observed under temperature modulation conditions.[4–6,20,24–27]

In addition, a small, truly reversible melting component is detected in the reversing endotherm in the absence of other irreversible processes such as recrystallization, annealing, and melting.[7,8,14–19] This is called "reversible melting" and it is expected to arise because of molecular nucleation, in which some of the molecules that have melted recrystallize onto the existing crystals with negligible cooling. This can be detected under the quasiisothermal (QI) mode (i.e., modulation about a constant temperature), which allows delaying measurements until the completion of other irreversible processes. The reversible melting phenomenon of PET, poly(oxyethylene),[10,11] and PEs[12–16] has been observed and the degree of reversibility has been quantified.

The interpretation of melting is usually based on the crystal structure of the polymer.[1] The crystals of semicrystalline polymers are never completely crystalline. They contain disordered regions and crystallites of varying sizes. Therefore, a partially crystalline polymer structure never stays in equilibrium and the extent of equilibration of the lamella structure can be studied by the way in which the lamella melts. The dimensions of crystallites depend on the polymer chain structure and prior thermal history. The lamella thickness is the main parameter that changes with the thermal history. When PE is cooled from the melt at relatively slow rates, the branches are excluded from the lamella. Long branches are excluded at the branch point, but the long branches can themselves take part in crystallization except when they contain short branches. The cooling rates and other conditions determine the extent to which molecular segments can segregate according to the length between branch points, so that each segment can crystallize with other segments of similar length to form the overall thickest distribution of lamella thicknesses.

In this research, the melting behavior of various PEs, high density PE (HDPE), low density PE (LDPE), linear low density PE (LLDPE), and very low density PE (VLDPE) was investigated by TMDSC. Various cooling programs were applied to obtain different crystal structures and morphologies. Since the evolution of the TMDSC technique, there have been many controversies over the TMDSC experimental conditions, data analysis, and data interpretation.[28,29] Two approaches are presently available for data analysis in terms of the reversing and nonreversing heat capacity[2] and complex heat capacity, which can be separated into in-phase and out of phase signals using the phase angle.[3] However, the problem associated with the complex heat capacity approach is the lack of interpretation of the out of phase component that is significantly influenced by the phase angle and thereby by the heat transfer effects.[30] Hence, the results here are presented and discussed using the reversing and nonreversing curves.

EXPERIMENTAL

Materials and preparation

The polymers used in this study are commercial PEs, and the characteristics of these polymers are presented in Table I. The HDPE and LDPE were supplied by Kemcor Australia Ltd. The LLDPE and VLDPE obtained from Qenos, Australia are single-site catalyzed ethylene-octene copolymers containing short and long branches. In order to reduce thermal lag during the analysis, flat, thin film samples (2–3 mg) were used. Films with about 100 μm thicknes were obtained by melt pressing the pellets in a heated press. The samples were encapsulated in aluminum pans with a crimper, and each polymer was heated to the melt at 180°C for 5 min to remove any prior thermal history before applying the thermal treatment. Four different crystallization methods were followed: slow cooling (SC2), fast cooling (FC50), modulated cooling (MC2), and isothermal crystallization (IC). The first two methods were cooling from the melt to 20°C in a DSC apparatus at constant rates of 2 and 50°C min^{-1}, respectively. The third method used a modulated cooling program (linear segments of cooling and heating in a TMDSC unit) with a cooling rate of 8°C min^{-1} for 30 s followed by heating at 4°C min^{-1} for 30 s from 150 to 20°C. This provided a temperature amplitude of 1.5°C, a frequency of 16.7 MHz, and an average cooling rate of 2°C min^{-1}. The fourth method was rapid cooling (200°C min^{-1}) to an isothermal crystallization temperature determined by adding 5°C to the onset temperature for crystallization, cooling at a constant rate of 2°C min^{-1}, holding for 1 h, and then cooling rapidly to 20°C.

TABLE I
Characteristics of Polymers

Properties	HDPE[a]	LDPE[a]	LLDPE[b]	VLDPE[b]
Comonomer	—	—	Octene	Octene
Catalyst type[c]		P	S	S
MFI (dg min^{-1})	0.3	20.0	1.0	1.0
Density (g cm^{-3})	0.953	0.918	0.915	0.908
M_w (g mol^{-1})			97800	96700
M_w/M_n		4.4	2.60	2.86
Comonomer content (wt %)	—	—	7.5	9.5
T_m (°C)[d]	130.1	103.9	111.3	107.5
T_c (°C)[d]	117.2	87.1	97.0	91.4

[a] Data were taken from chemical data sheets published by the manufacturer.
[b] Reference 31.
[c] S, constrained geometry single-site catalyst; P, peroxide.
[d] Crystallization (T_c) and melting (T_m) temperatures were obtained at scanning rates of 10°C min^{-1}.

DSC measurements

All measurements and thermal treatments were performed on a Perkin–Elmer Pyris 1 dynamic differential scanning calorimeter (DDSC) under a dry nitrogen purge at 15 mL min^{-1}. The DDSC was operated at subambient temperature mode with a refrigerated cooling system (Intracooler 2P, −65°C). The calorimeter was calibrated for temperature using cyclohexane, indium, and zinc standards and a furnace calibration was performed. The temperature calibration was checked regularly against the melting onset temperature of indium. The heat flow calibration was performed using indium. A thin film of a relatively small sample mass of about 2 mg was used to minimize thermal lag. Standard DSC heating and cooling scans were performed at a rate of 10°C min^{-1} and the DSC data are listed in Table I. TMDSC melting scans of thermally treated samples were immediately obtained by using a saw-tooth modulation from 25 to 150°C. The underlying heating rate was set to 2°C min^{-1} with a temperature amplitude of 1.5°C and an oscillation frequency of 16.7 MHz. The baseline scan was performed using matched empty pans under the same conditions. The average heat flow data over one cycle from the DDSC scans were then used to calculate the total heat capacity (total C_p). The values of C_p' and C_p' were calculated using the Perkin–Elmer software according to the method of Schawe.[3] The C_{pNR} curve was obtained by subtracting the C_p' curve from the total C_p curve. The QI mode experiments (16.7-MHz oscillation frequency, 0.5°C temperature amplitude, and zero underlying heating rate) were carried out as described by Ishikiriyama and Wunderlich.[11] The crystallinity was calculated from the enthalpy of the total heat flow endotherms taken from 35 to 135°C. The heat of fusion (ΔH) value for 100% crystalline PE was taken as 293 J g^{-1}.[32]

RESULTS AND DISCUSSION

Melting of HDPE

Figure 1 displays the specific heat melting curves obtained for HDPE after each of the four thermal histories, and Table II lists the melting characteristics for each of the polymers. The total C_p curves of HDPE obtained after slow cooling, modulated cooling, fast cooling, and isothermal crystallization treatments (I–IV) are given in Figure 1(a). All curves show relatively narrow, single melting endothermic peaks, with the SC2-HDPE sample displaying the sharpest peak. As mentioned earlier, the total C_p curve, which is obtained by averaging the heat flow, is equivalent to the normal DSC curve recorded using the same average heating rate. In order to further elucidate the changes taking place during melting, it is necessary to consider the dynamic components of the TMDSC curves. Figure 1(b) shows the C_p' curves, which are expected to reveal the component of melting that is reversible at the time and temperature of the experiment. All of the C_p' curves clearly exhibit a broad double melting endotherm starting from about 60°C to the main melting peak. The peak melting temperatures of C_p' ($T_{mCp'}$) do not correspond to those of the total C_p curves and are slightly shifted to a higher temperature (see Table II).

The nonreversing curves illustrated in Figure 1(c) also show relatively sharp endothermic peaks similar to the total C_p curves, indicating that some of the melting has taken place irreversibly under the conditions of the measurements. Analogous curves have also been observed by Cser et al.[33] for a similar HDPE, which was continuously cooled at 2°C min^{-1} from the melt followed by analysis at a 2°C min^{-1} underlying heating rate in a modulated DSC calorimeter. All of the C_{pNR} curves developed an initial deviation from zero at about 100°C, indicating that no irreversible changes were occurring below 100°C. Therefore, most

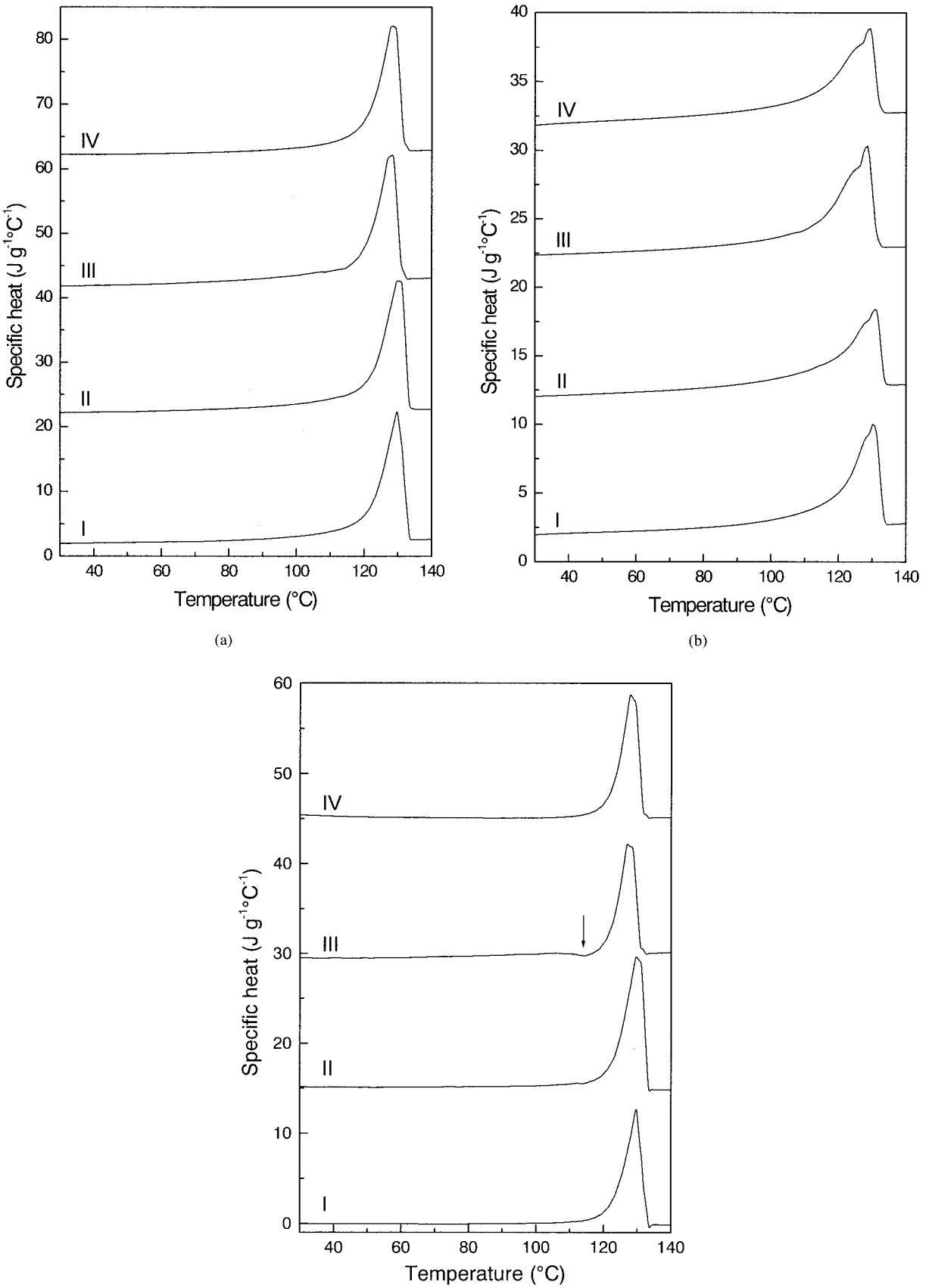

Figure 1 Modulated specific heat curves of HDPE samples crystallized after different conditions: (a) total specific heat curves, (b) reversing specific heat curves, and (c) nonreversing specific heat curves. The crystallization conditions involved slow cooling at 2°C min^{-1} (curve I), dynamic cooling at an average rate of 2°C min^{-1} (curve II), fast cooling at 50°C min^{-1} (curve III), and isothermal crystallization at 127°C for 30 min (curve IV). An adapted scale is drawn by consecutively adding 20, 10, and 15 units to each series of curves for the total, reversing, and nonreversing curves, respectively.

TABLE II
TMDSC Data of Polymers after Different Crystallization Conditions

Polymer	T_m (total) (°C)	ΔH_m (Total) (J g^{-1})	T_m (C_p') (°C)	ΔH_m (C_p') (J g^{-1})	T_m ($C_{p\mathrm{NR}}$) (°C)	ΔH_m ($C_{p\mathrm{NR}}$) (J g^{-1})	χ
IC-HDPE	128.2	178.8	129.3	98.7	127.9	80.1	0.62
FC50-HDPE	128.4	182.3	128.6	109.1	127.0	73.2	0.63
MC2-HDPE	129.9	208.3	131.1	86.1	129.7	122.2	0.72
SC2-HDPE	129.7	181.9	130.2	95.4	129.7	86.5	0.63
IC-LDPE	103.6	92.7	102.9	90.9	105.6	1.79	0.32
FC50-LDPE	105.2	95.9	103.9	86.5	105.2, 107.3	9.5	0.33
MC2-LDPE	105.1	106.1	104.3	75.0	105.1	31.0	0.37
SC2-LDPE	105.7	101.1	104.1	71.6	103.6	29.5	0.35
IC-LLDPE	109.7	101.9	110.0	104.4	109.7	−2.45	0.35
FC50-LLDPE	111.1	107.5	109.9	104.6	111.3	2.9	0.37
MC2-LLDPE	111.3	129.7	109.9	78.6	111.2	51.1	0.45
SC2-LLDPE	111.4	112.3	110.2	82.5	111.5	29.8	0.39
IC-VLDPE	105.8, 99.6	96.2	106.2	84.6	105.7	11.7	0.33
FC50-VLDPE	106.5	85.6	105.1	103.7	106.8	−15.1	0.30
MC2-VLDPE	107.0	112.5	101.7, 107.9	53.1	107.0	59.3	0.39
SC2-VLDPE	107.4	86.5	106.3	99.4	107.5	−12.9	0.30

of the crystallization and annealing processes providing the broadness seen in the C_p' curve must be occurring during the melting range because no evidence of an irreversible change is observed in the $C_{p\mathrm{NR}}$ curve before the main melting peak. Nevertheless, the $C_{p\mathrm{NR}}$ curve of FC50-HDPE showed a small exothermic peak at ~114°C prior to melting [Fig. 1(c), arrow], suggesting that the recrystallization and annealing of crystallites proceeded on heating as a consequence of the unstable crystals formed by the fast cooling treatment at 50°C min^{-1}. The recrystallization exotherm started immediately after the partial melting of the initial crystals at a lower temperature. Therefore, the process of melting, recrystallization, and remelting (MRR) occurs in this sample; and the reversing curve corresponds to the melting of primary and remelting of secondary crystals. Conversely, the HDPE sample crystallized at a slow cooling rate (2°C min^{-1}) had a sharp melting peak and showed no visible exothermic transition in the $C_{p\mathrm{NR}}$ curve. Moreover, the slight bimodal melting behavior seen in all C_p' curves of Figure 1(b) may be attributed to the process of crystal annealing. The average heating rate used here to obtain the melting scan of treated polymers was 2°C min^{-1}, and there was a possibility of crystal annealing at a such a slow heating rate. Because melting was dominant in this temperature range, no exothermic activity related to annealing was detected during the experimental time scale.

As seen in Table II, the melting temperatures (T_m) of HDPE crystallized by continuous and modulated cooling at a rate of 2°C min^{-1} (curves I, II) were higher than those of fast cooled and isothermally crystallized HDPE. The MC2-HDPE had the highest crystallinity ($\chi = 0.72$) and the isothermally crystallized sample at 127°C had the lowest value (0.62) of all. However, the slowly cooled HDPE had the sharpest and narrowest endothermic peak, indicative of the presence well-organized lamellae [refer to Fig. 1(a)]. Modulated cooling in a TMDSC has been known to anneal polymer crystals. Menzel[34] found that modulated cooling can be used to enhance the perfection of poly(*p*-phenylene sulfide) crystals formed during the conventional cooling from the melt, and the perfection was significantly improved by remelting and recrystallization of the outer lamella layers. Thus, the increased T_m and crystallinity of MC2-HDPE could be attributed to crystal perfection during the modulated cooling.

It is also interesting to note that the enthalpy of the C_p' endotherm of FC50-HDPE was considerably larger than that of the $C_{p\mathrm{NR}}$ endotherm. It is known that poorly crystallized polymers have a larger reversing melting contribution, whereas perfect crystals show little or none.[4,35] Therefore, the larger reversing contribution of FC50-HDPE verifies the formation of thermally unstable crystals. In contrast, the MC2-HDPE sample had the largest nonreversing melting (122.2 J g^{-1}) and the smallest reversing component (86.1 J g^{-1}), a characteristic of the melting of thermally stable crystals.

Melting of LDPE

Figure 2(a) shows the total C_p curves for LDPE, and the melting endotherms reveal a complex pattern of closely spaced peaks. Melting started at a temperature as low as 50°C and a broad low melting region preceded the main melting peaks. Two overlapped peaks were seen for the SC2-LDPE (103.7 and 105.1°C) and MC2-LDPE (103.6 and 105.1°C) samples, and three peaks were detected for the FC50-LDPE (103.5, 105.2, and 106.8°C) and IC-LDPE samples (101.9, 103.6, and 105.2°C). The C_p' curves shown in Figure 2(b) emphasize the low temperature melting region (35–105°C),

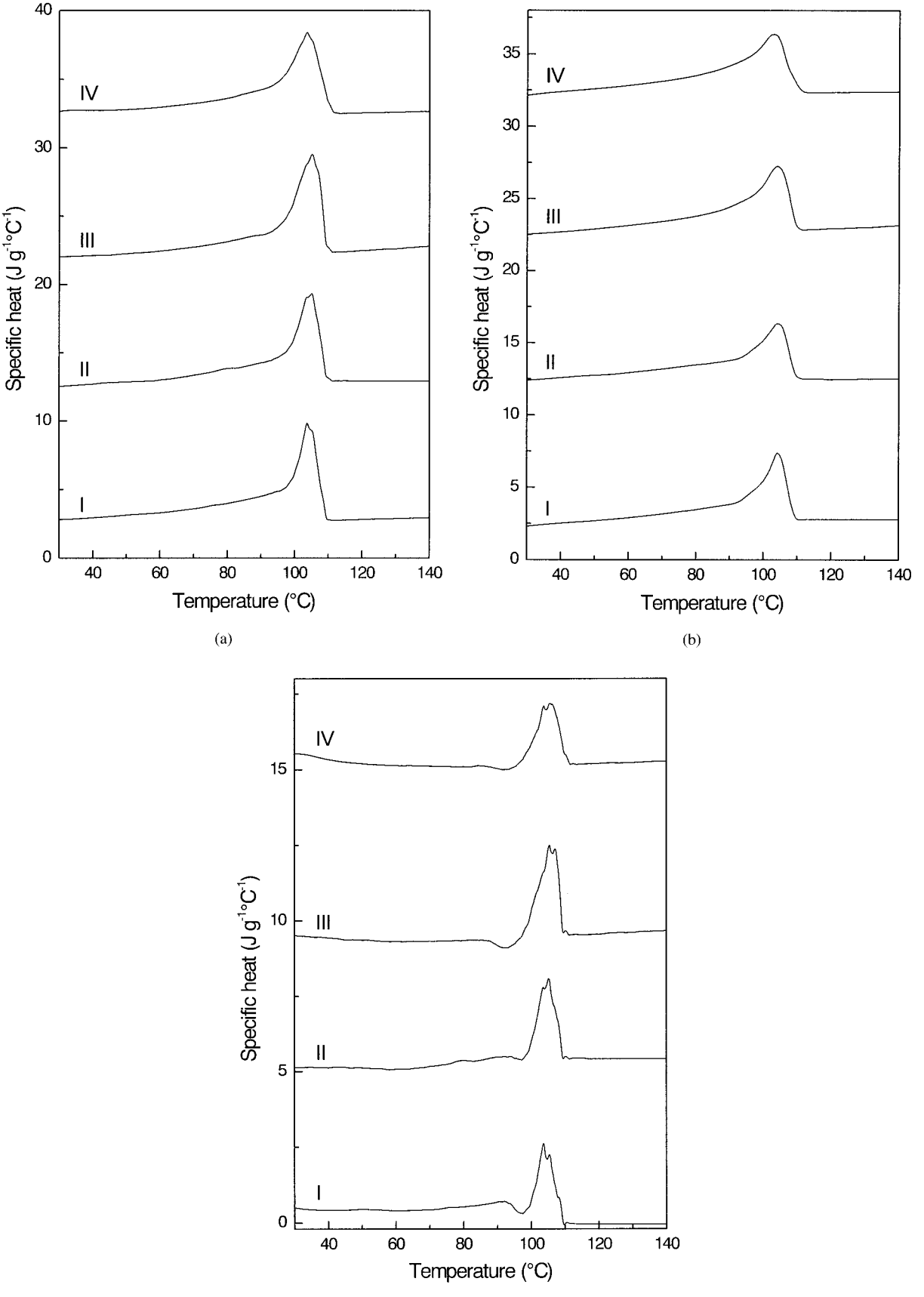

Figure 2 Modulated specific heat curves of LDPE samples crystallized after different conditions: (a) total specific heat curves, (b) reversing specific heat curves, and (c) nonreversing specific heat curves. The crystallization conditions involved slow cooling at 2°C min^{-1} (curve I), dynamic cooling at an average rate of 2°C min^{-1} (curve II), fast cooling at 50°C min^{-1} (curve III), and isothermal crystallization at 102°C for 30 min (curve IV). An adapted scale is drawn by consecutively adding 10, 10, and 5 units to each series of curves for the total, reversing, and nonreversing curves, respectively.

but the main melting peak is much broader and the T_m values are much lower than those of the total C_p curves. The $C_{p\mathrm{NR}}$ curves are shown in Figure 2(c), and this is the component where complex multiple peaks are exhibited. Each of the curves contains several overlapped peaks, and all the thermal treatments on LDPE showed an exotherm (90–100°C) just before the main melting endotherm. The double or multiple melting behavior is not uncommon for branched PEs, depending on the structure and crystallization conditions. It is proposed to link to either the process of MRR or structural heterogeneity.[36] As mentioned previously, the $C_{p\mathrm{NR}}$ curves showed the exothermic transition just before the main melting, suggesting the crystals undergo recrystallization during heating. The recrystallization exotherm started immediately after the melting of the initial crystals at a lower temperature. Nonetheless, a double melting reversing endothermic peak, in conjunction with a recrystallization exothermic nonreversing contribution, was observed for isothermally crystallized PEs,[13] PET,[37] and syndiotactic polystyrene.[38] Furthermore, such a transition is often impossible to detect in the conventional DSC scan because of the offset of the recrystallization exotherm and the melting endotherm.

All the reversing heat capacity contributions were higher than those of the nonreversing contributions. The IC-LDPE sample showed the highest reversing component, indicating that more thermally unstable crystals had been formed during the fast cooling that followed isothermal crystallization at 102°C. As seen earlier in the case with HDPE, MC2-LDPE had the highest crystallinity, which was attributed to thickening of the lamellar surfaces. LDPE contains both short and long branches. Thus, the crystallization would be greatly affected by the branches and a distribution of thin and thick lamellae can be observed. These crystals are known to undergo crystallization and annealing and this has been verified by the exotherm observed in the $C_{p\mathrm{NR}}$ curve before the melting. Thus, the observed behavior is attributed to the highly branched character of LDPE. In addition, the TMDSC scans reveal that all LDPEs experience melting processes such as crystallization and annealing, regardless of the crystallization conditions.

Melting of LLDPE

Behavior analogous to LDPE was observed for LLDPE, which is an ethylene-octene copolymer having both short and long branches. The specific heat curves shown in Figure 3(a–c) are similar to those for LDPE with the peak melting temperatures being higher than those of LDPE. Again, melting started at a low temperature of about 50°C and continued with heating toward the main melting peak. The total C_p endotherms [Fig. 3(a)] show double peaks, except for the MC2-LLDPE that consists of a sharp single peak. Figure 3(b) displays the C_p' curves and broader melting endotherms, virtually starting from room temperature, are observed. The reversing melting contribution, which was measured under the particular experimental conditions, seemed to predominate over the lower temperatures of the melting range. The $C_{p\mathrm{NR}}$ curves [Fig. 3(c)] showed the presence of complex unresolved melting peaks, except for MC2-LLDPE, which exhibited a sharp single peak. Moreover, all the LLDPE curves, except SC2-LLDPE, showed an exothermic transition before the main melting, suggesting the crystallites that are formed experience crystallization and annealing before melting. It was also noticed that FC50-LLDPE had the largest reversing contribution and an exothermic transition in the $C_{p\mathrm{NR}}$ curve, reflecting that cooling at a 50°C min^{-1} rate formed unstable crystallites. Similar to the other polymers, MC2-LLDPE had the highest crystallinity because of the crystal perfection at the crystal surface.

Nam et al.[35] studied the structural changes of LLDPE by small angle X-ray scattering (SAXS) and TMDSC during the heating process. They also observed a broad, large reversing peak and a small, sharp nonreversing peak, suggesting continuous melting of a large fraction of thermally unstable thin lamellae that formed over a wide temperature range during cooling. Furthermore, their morphological observation by SAXS revealed that this disordering was caused by the melting of thin lamellae existing between thicker lamellae that had developed at higher temperatures. The LLDPE studied here is a single-site catalyzed polymer with 7.5 wt % comonomer content, which provides a high branch content. It has been found that LLDPE contains finer lamellar crystals and spherulitic morphology; and, upon cooling, a range of thick and thin lamellae is formed.[39]

Melting of VLDPE

The melting behavior of a VLDPE prepared by single-site catalyst technology after TMDSC analysis is shown in Figure 4(a–c). VLDPE has a more branched character (9.5 wt %) than LLDPE and is therefore it expected to contain mostly fringed-micellar structures.[39] The observed melting endotherms are parallel to those obtained for highly branched LDPE. Multiple melting peaks in the total C_p curves are observed but not resolved. The C_p' curves [Fig. 4(b)] had broad endotherms, showing only a double melting peak for IC-VLDPE. The reversing peak begins at a temperature as low as 35°C and continues to the main melting peak. Figure 4(c) shows the $C_{p\mathrm{NR}}$ specific heat curves in which multiple melting endotherms are prevalent, which are mostly obscured in the total specific heat curve. Again, the exothermic transformation before the main melting peak in the $C_{p\mathrm{NR}}$ curves indicates

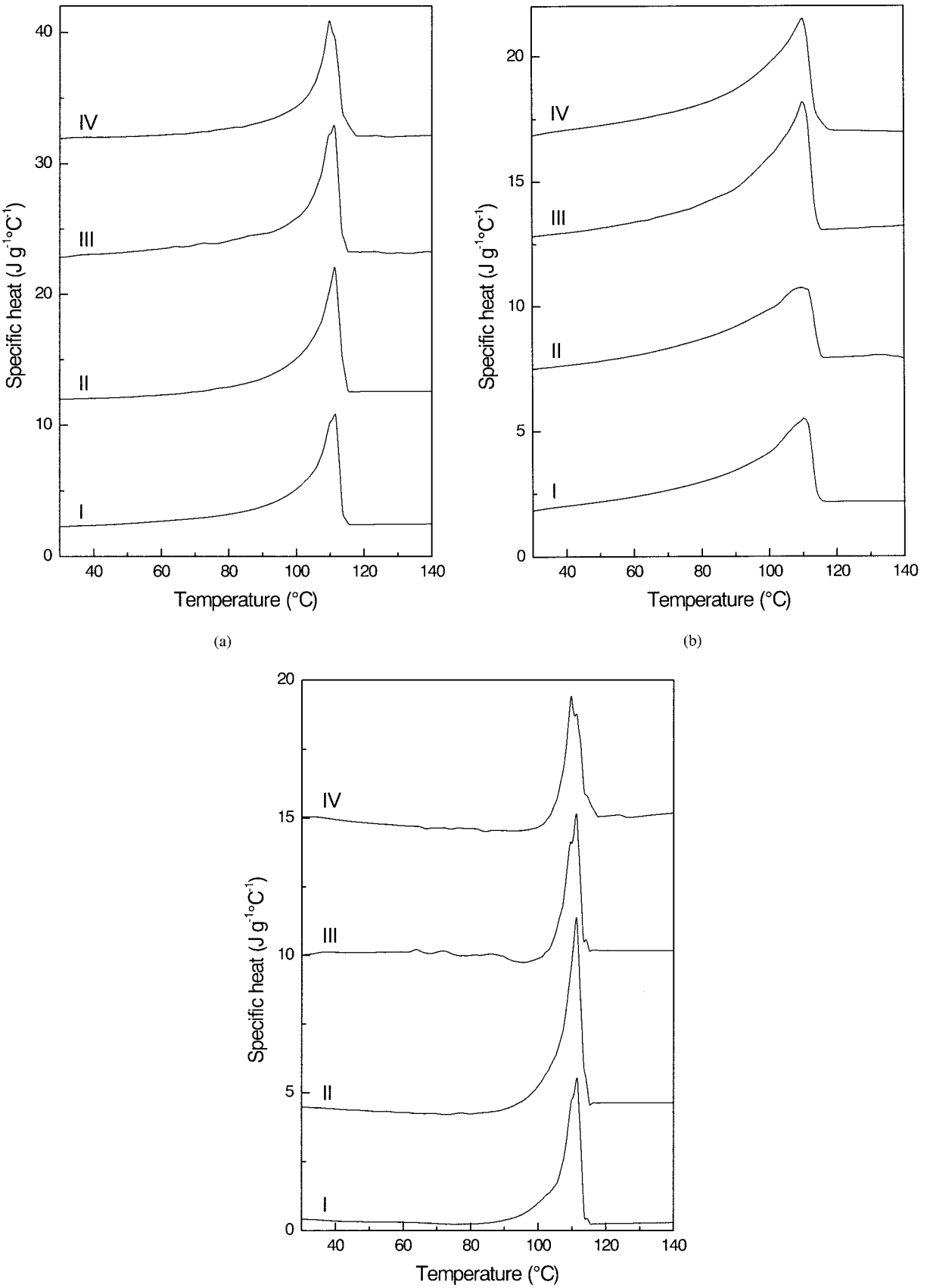

Figure 3 Modulated specific heat curves of LLDPE samples crystallized after different conditions: (a) total specific heat curves, (b) reversing specific heat curves, and (c) nonreversing specific heat curves. The crystallization conditions involved slow cooling at 2°C min^{-1} (curve I), dynamic cooling at an average rate of 2°C min^{-1} (curve II), fast cooling at 50°C min^{-1} (curve III), and isothermal crystallization at 110°C for 30 min (curve IV). An adapted scale is drawn by consecutively adding 10, 5, and 5 units to each series of curves for the total, reversing, and nonreversing curves, respectively.

that recrystallization and annealing occur while the sample is continuously heated. This trend is similar to the other crystallized polymers we observed, FC50-VLDPE being the least and MC2-VLDPE being the most stable. FC50-VLDPE has the largest reversing contribution with a negative $C_{p\mathrm{NR}}$ contribution, and MC2-VLDPE has the smallest reversing component with the largest $C_{p\mathrm{NR}}$ contribution. In addition, for all VLDPE samples, a very small or negative $C_{p\mathrm{NR}}$ contribution is observed.

It is known that PE crystals become thicker during isothermal crystallization, shifting the T_m value to a higher temperature. Melting of VLDPE after isothermal crystallization at 103.2°C gave two well-defined peaks and the lower temperature peak was from the crystals that formed during the rapid cooling to room temperature [Fig. 4(a), curve IV]. Because the rapidly cooled crystals are metastable, they experience crystallization and annealing as depicted by the exothermic change before the melting in the $C_{p\mathrm{NR}}$ curve. Similar melting behavior was reported by Janimak and Stevens for other single-site catalyzed PEs.[13] In their studies, a double melting reversing endothermic peak, in conjunction with an exothermic nonreversing contribution, was observed for the PE having a melting temperature of 116°C, which was isothermally crystallized at 115°C for 1 h following rapid or slow cooling to room temperature.

Comparison of melting of PEs

The relative magnitude of the reversing and nonreversing contributions differs between the PE types. HDPE exhibits reversing and nonreversing endotherms of nearly the same ΔH value (Table II). LDPE, LLDPE, and VLDPE each showed mainly reversible melting, particularly for the isothermal and fast cooled samples. Slow and modulated cooling allowed better equilibration of the crystals, which increased the nonreversible contribution. Modulated cooling over all of the PEs provided the highest amounts of nonreversible melting and provides the conditions for crystallization and lamella thickening in the same temperature scan. Isothermal cooling gave low or negative nonreversing ΔH values for LDPE, LLDPE, and VLDPE, whereas fast and slow cooling gave negative nonreversing ΔH values for VLDPE. The negative ΔH values were the result of a broad exotherm prior to the main melting peak. The exotherm was canceled in the total C_p curves by a broad endotherm at the start of melting in the reversing curves. This endotherm–exotherm combination can be attributed to the MRR of the PEs prior to the main melting region. This is supported by such recrystallization being greater for the more branched PEs and where crystallization conditions were likely to lead to poorly formed crystals. Alternatively, the negative $C_{p\mathrm{NR}}$ could be an artifact of the method where C_p' may be overestimated, resulting in a negative $C_{p\mathrm{NR}}$ because it is calculated from a difference. However, nonlinearity and lack of stationary conditions are less likely in the premelt range; they are more likely to occur in the temperature range where melting is fastest. This can be demonstrated by Lissajous figures of the various temperature regions.

QI TMDSC analysis

As previously mentioned, the C_p' curve characterizes only part of the reversible events under the modulation conditions. QI TMDSC experiments have recently been used to probe and quantify processes that are truly reversible.[14–19] The QI TMDSC specific heat capacity curves, measured at various temperatures over the melting range after a modulation for 20 min at a constant temperature, are shown in Figure 5(a,b). After removing all modulation distortions due to the irreversible effects (i.e., achieving the steady state), the curve shows only relatively small reversing contributions for FC50-HDPE and SC2-HDPE as shown in Figure 5(a). The approach to the steady state was checked by constructing Lissajous figures.[40] The good agreement between the heat capacities before and after melting suggests that melting is mostly thermodynamically reversible in these regions. The standard DSC curve (thin line) contains many effects, including the reversible melting. However, the reversible contribution of SC2-HDPE within the melting range was a very minor portion (18.5%) of the total curve. Such a small amount of reversible melting contributions has been observed for other PEs.[14,15] Furthermore, the enthalpy of slowly cooled HDPE (38.2 J g^{-1}) was slightly less than that of fast cooled HDPE (41.0 J g^{-1}). The enthalpy was calculated by integrating the C_p' curve over the analyzed temperature range. The degree of reversibility was very low for the relatively perfect lamellae of highly crystalline HDPE. In contrast, polymers of low crystallinity, in which lamellae are not the prevalent crystal morphology, show a higher degree of reversibility. Such is the case observed in Figure 5(b), in which FC50-VLDPE shows a relatively higher reversing heat capacity. The fraction of the reversible contribution of SC2-VDPE within the melting range was 33.5%. In this case, the enthalpy of FC50-VLDPE (35.9 J g^{-1}) was significantly higher than that of SC2-VLDPE (30.3 J g^{-1}), suggesting the higher degree of reversibility in the quickly cooled sample.

Final assessments

When PEs are crystallized, molecular chains are folded into lamella structures that are controlled by the branch content and distribution. Because HDPE has virtually no branches to restrict the incorporation of chain segments into the crystals, the lamellae are

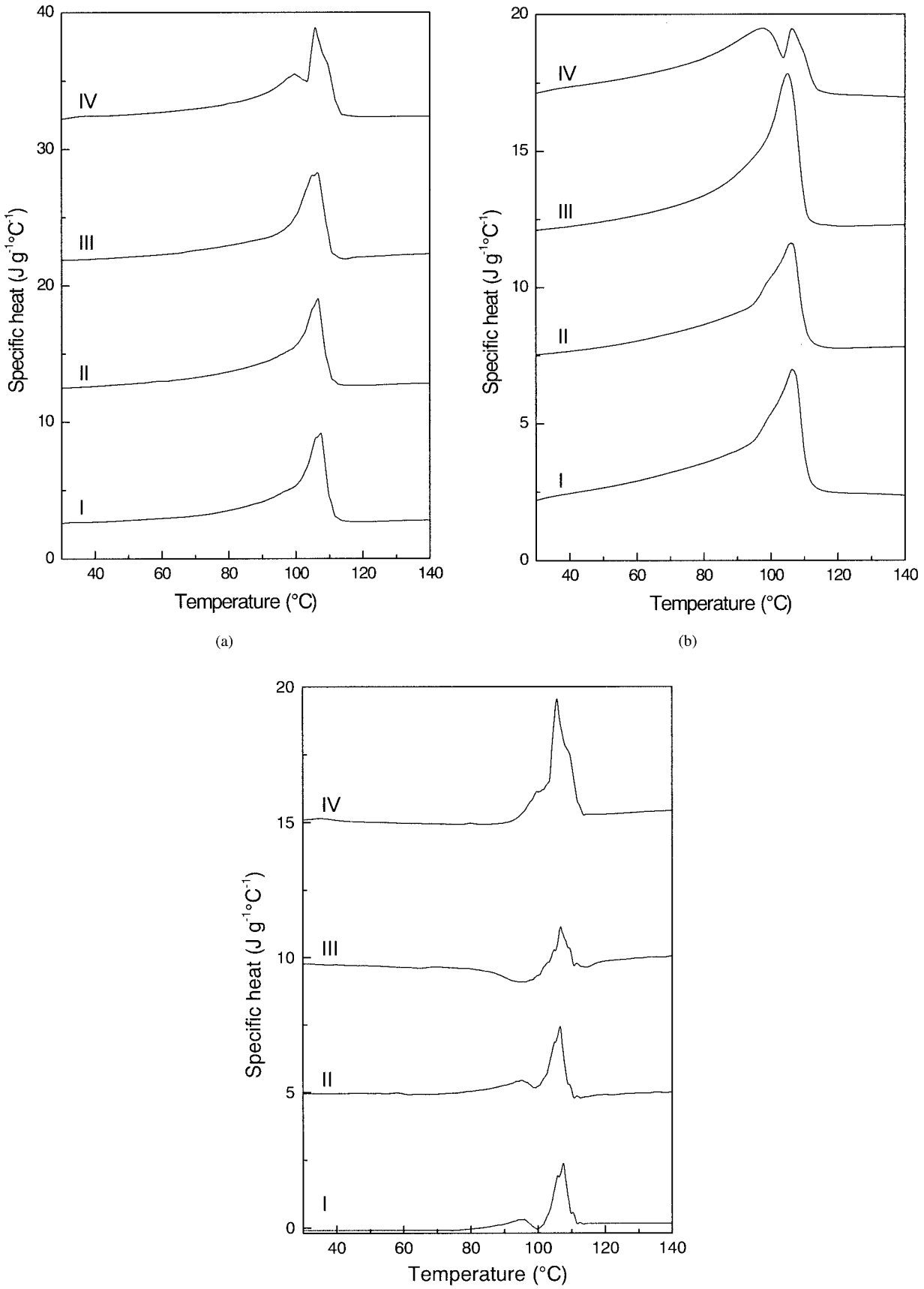

Figure 4 Modulated specific heat curves of VLDPE samples crystallized after different conditions: (a) total specific heat curves, (b) reversing specific heat curves, and (c) nonreversing specific heat curves. The crystallization conditions involved slow cooling at 2°C min^{-1} (curve I), dynamic cooling at an average rate of 2°C min^{-1} (curve II), fast cooling at 50°C min^{-1} (curve III), and isothermal crystallization at 103°C for 30 min (curve IV). An adapted scale is drawn by consecutively adding 10, 5, and 5 units to each series of curves for the total, reversing, and nonreversing curves, respectively.

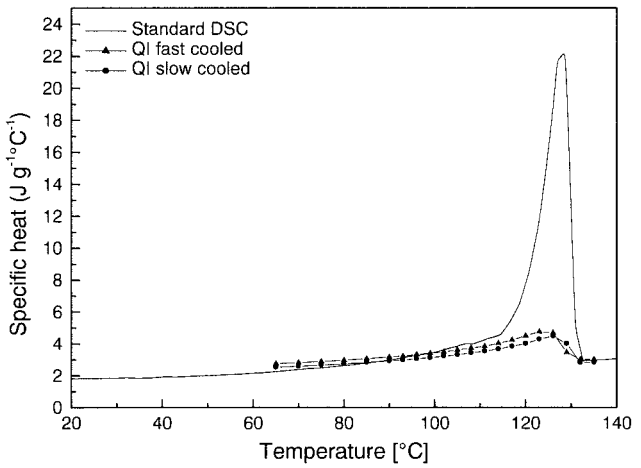

Figure 5 Quasiisothermal modulated specific heat curves of (a) HDPE and (b) VLDPE. Measurements are performed in the 50–122°C range with 2–5°C steps. The modulation parameters are an underlying 0°C min^{-1} heating rate, 0.5°C temperature amplitude, 60-s period, and 20-min duration. The last 10 min of modulation data are used for the calculation. (—) The standard DSC curve obtained at a 10°C min^{-1} rate.

well organized. In contrast, the branches in LDPE, LLDPE, and VLDPE restrict crystallization, depending on the branch density. LLDPE and VLDPE are copolymers and have partial lamella structures that contain a mixture of lamella and bundlelike crystals.[39] The thermal history determines how well the lamella crystals and surfaces organize in these polymers. The sequence of crystallization events of homopolymers and copolymers under isothermal conditions has been observed by Mirabella.[41] In the case of homopolymers (HDPE), thinner crystals are expected to form first and then thickening of the crystals will occur later. Conversely, the formation of thicker crystals, followed by secondary crystallization to form thinner crystals, is observed for the copolymers.

Melting of each of the PEs after the different thermal histories provides interesting observations when the total melting endotherms are divided into their reversing and nonreversing components. The relative fraction of reversing and nonreversing components depends on the crystal type and the experimental conditions. The reversing contribution is always broader and smaller in magnitude than the total C_p. It originates at a lower temperature than the $C_{p\mathrm{NR}}$ heat capacities, so this is the main contributor to the lower temperature melting observed in the total specific heat curve. Molecules melting at lower temperatures can recrystallize because these molecules melt at temperatures that are far below their true melting temperatures, except when they are of the fraction with the highest branching density. A slow rate of crystallization usually promotes more perfect crystals, which have higher melting temperatures. These crystals recrystallize or anneal less on heating. Conversely, low melting crystals with defects are formed upon fast cooling. The exothermic changes in the $C_{p\mathrm{NR}}$ traces of fast cooled samples provided evidence for crystallization that occurred in parallel with melting. However, such crystallization is not observed for the slowly cooled samples, except in cases where the polymer is highly branched (LDPE and VLDPE). Nonetheless, thermally fractionated samples of branched LLDPE and VLDPE, which are crystallized at an average rate of 0.08°C min^{-1} by stepwise cooling (50-min isothermal step at every 4°C), show no recrystallization during melting with similar modulation parameters.[42] Under this condition, these samples are expected to form nearly equilibrium crystals after the complete segregation of molecular segments.

The presence of multiple endotherms also raises the question as to whether they are due to MRR or structural heterogeneity. Multiple melting endotherms are usually seen in the melting curves of LLDPE because of structural heterogeneity (i.e., a broad and multimodal short chain branch distribution).[36] The TMDSC data reveal that the recrystallization exotherm is indicative of MRR and the multiple melting behavior seen in LDPE, LLDPE, and VLDPE may be attributed to the process of MRR. However, the recrystallization exotherm cannot be taken for any quantitative measurements, because the $C_{p\mathrm{NR}}$ curves also contain other irreversible effects.

Wunderlich and coworkers have suggested six contributions to heat capacity, three reversible and three irreversible: thermodynamic heat capacity, heat capacity due to conformational motions, reversible melting, crystal perfection, secondary crystallization, and primary crystallization.[14–19] A small amount of reversible melting was seen during the melting of HDPE and VLDPE. Reversible melting is a minor component of the total melting, and the thermodynamic heat capacity and heat capacity due to conformational motions

include the major portion. The degree of reversibility of fast cooled polymers was also found to be higher than that of slow cooled polymers. In addition, the HDPE with no branches undergoes less reversible melting and crystallization compared to VLDPE with many branches. All these data imply that the reversible melting depends on the polymer chain structure and morphology, as suggested by Androsch and Wunderlich for ethylene-octene copolymers.[14,15] Although the interpretation of TMDSC data is dependent on the experimental conditions (mainly modulation parameters), it provides important qualitative results that are useful in characterizing polymers.

CONCLUSION

The TMDSC results of the polymers are strongly dependent on the prior thermal treatments. It was found that crystals formed under different crystallization conditions had different structures; hence, they showed different amounts of reversing and nonreversing contributions. The data showed that the lamellae of all branched PEs (LDPE, LLDPE, and VLDPE) prepared at various conditions were rearranged before they melted. In the case of HDPE, only fast cooled HDPE showed melting and crystallization. The crystallinity indicated that dynamically cooled polymers were much more crystalline, which can be attributed to crystal perfection at the lamella surface. The main melting is irreversible, but some reversible contributions are observed by QI TMDSC measurements. The melting of PEs is complicated because of reorganization and/or recrystallization during melting, and the results showed that TMDSC could provide some insight into the kinetics and mechanism of melting.

References

1. Wunderlich, B. Crystal Melting, Macromolecular Physics; Academic: New York, 1980; Vol. 3, p 128.
2. Gill, P. S.; Sauerbrunn, S. R.; Reading, M. J Therm Anal 1993, 40, 931.
3. Schawe, J. E. K. Thermochim Acta 1995, 260, 1.
4. Wunderlich, B.; Okazaki, I.; Ishikiriyama, K.; Boller, A. Thermochim Acta 1998, 324, 77.
5. Wunderlich, B.; Boller, A.; Okazaki, I.; Ishikiriyama, K.; Chen, W.; Pyda, M.; Pak, J.; Moon, I.; Androsch, R. Thermochim Acta 1999, 330, 21.
6. Simon, S. L. Thermochim Acta 2001, 374, 55.
7. Okazaki, I.; Wunderlich, B. Macromol Rapid Commun 1997, 18, 313.
8. Okazaki, I.; Wunderlich, B. Macromolecules 1997, 30, 1758.
9. Schick, C.; Merzlyakov, M.; Wunderlich, B. Polym Bull 1998, 40, 297.
10. Ishikiriyama, K.; Wunderlich, B. Macromolecules 1997, 30, 4126.
11. Ishikiriyama, K.; Wunderlich, B. J Polym Sci Polym Phys 1997, 35, 1877.
12. Scherrenberg, R.; Mathot, V.; Van Hemelrjk, A. Thermochim Acta 1999, 330, 3.
13. Janimak, J. J.; Stevens, G. C. Thermochim Acta 1999, 332, 125.
14. Androsch, R.; Wunderlich, B. Macromolecules 1999, 32, 7238.
15. Androsch, R.; Wunderlich, B. Macromolecules 2000, 33, 9076.
16. Pak, J.; Wunderlich, B. Macromolecules 2001, 34, 4503.
17. Androsch, R.; Wunderlich, B. Macromolecules 2001, 34, 5950.
18. Androsch, R.; Wunderlich, B. Macromolecules 2001, 34, 8384.
19. Pyda, M.; Di Lorenzo, M. L.; Pak, J.; Kamasa, P.; Buzin, A.; Grebowicz, J.; Wunderlich, B. J Polym Sci Polym Phys 2001, 39, 1565.
20. Sauer, B. B.; Kampert, W. G.; Neal Blanchard, E.; Threefoot, S. A.; Hsiao, B. S. Polymer 2000, 41, 1099.
21. Kampert, W. G.; Sauer, B. B. Polymer 2001, 42, 8703.
22. Di Lorenzo, M. L.; Pyda, M.; Wunderlich, B. J Polym Sci Polym Phys 2001, 39, 2969.
23. Reading, M.; Luyt, R. J. J Therm Anal 1998, 54, 535.
24. Toda, A.; Tomita, C.; Hikosaka, M.; Saruyama, Y. Polymer 1998, 21, 5053.
25. Toda, A.; Tomita, C.; Hikosaka, M.; Saruyama, Y. Thermochim Acta 1998, 324, 95.
26. Androsch, R. Polymer 1999, 40, 2805.
27. Pyda, M.; Wunderlich, B. J Polym Sci Polym Phys 2000, 38, 622.
28. Hill, V. L.; Craig, D. Q. M.; Feely, L. C. Int J Pharm 1999, 192, 21.
29. Jiang, Z.; Imire, C. T.; Hutchinson, J. M. Thermochim Acta 2002, 387, 75.
30. Righetti, M. C. Thermochim Acta 1999, 330, 131.
31. Schellenberg, J.; Wagner, B. J Therm Anal Calorim 1998, 52, 275.
32. Wunderlich, B. Crystal Melting, Macromolecular Physics; Academic: New York, 1980; Vol. 3, p 48.
33. Cser, F.; Rasoul, F.; Kosior, E. J Therm Anal 1998, 52, 293.
34. Menzel, J. D. J Therm Anal Calorim 1999, 58, 517.
35. Nam, J. Y.; Kadomatsu, S.; Saito, H.; Inoue, T. Polymer 2002, 43, 2101.
36. Mathot, V. B. F. Calorimetry and Thermal Analysis of Polymers; Hanser: New York, 1993; p 232.
37. Yuan, Z.; Song, R.; Shen, D. Polym Int 2000, 49, 1377.
38. Wunderlich, B.; Boller, A.; Okazaki, I.; Kreitmeier, A. Thermochim Acta 1996, 282/283, 143.
39. Bensason, S.; Minick, J.; Moet, A.; Chum, S.; Hiltner, A.; Baer, E. J Polym Sci Polym Phys 1996, 34, 1301.
40. Amarasinghe, G.; Shanks, R. A. unpublished results.
41. Mirabella, F. M. J Polym Sci Polym Phys 2001, 39, 2800.
42. Amarasinghe, G.; Shanks, R. A., submitted.